THE ROYAL SOCIETY

Received 11 May 2004
Accepted 7 July 2004
Published online 20 October 2004

Adhesion forces measured at the level of a terminal plate of the fly's seta

Mattias G. Langer[1], J. Peter Ruppersberg[2] and Stanislav Gorb[3,4*]

[1]*Sensory Biophysics Group, Department of Applied Physiology, University of Ulm, Albert-Einstein-Allee 11, 89081 Ulm, Germany*
[2]*Hearing Research Centre, Division of Sensory Biophysics, Department of Otolaryngology, University of Tübingen, Elfriede-Aulhorn-Strasse 5, D-72076 Tübingen, Germany*
[3]*Biological Microtribology Group, Biochemistry Department, MPI of Developmental Biology, Spemannstrasse 35, D-72076 Tübingen, Germany*
[4]*Evolutionary Biomaterials Group, Max-Planck-Institute for Metals Research, Heisenbergstrasse 3, D-70569 Stuttgart, Germany*

The attachment pads of fly legs are covered with setae, each ending in small terminal plates coated with secretory fluid. A cluster of these terminal plates contacting a substrate surface generates strong attractive forces that hold the insect on smooth surfaces. Previous research assumed that cohesive forces and molecular adhesion were involved in the fly attachment mechanism. The main elements that contribute to the overall attachment force, however, remained unknown. Multiple local force–volume measurements were performed on individual terminal plates by using atomic force microscopy. It was shown that the geometry of a single terminal plate had a higher border and considerably lower centre. Local adhesion was approximately twice as strong in the centre of the plate as on its border. Adhesion of fly footprints on a glass surface, recorded within 20 min after preparation, was similar to adhesion in the centre of a single attachment pad. Adhesion strongly decreased with decreasing volume of footprint fluid, indicating that the layer of pad secretion covering the terminal plates is crucial for the generation of a strong attractive force. Our data provide the first direct evidence that, in addition to Van der Waals and Coulomb forces, attractive capillary forces, mediated by pad secretion, are a critical factor in the fly's attachment mechanism.

Keywords: adhesion; attachment pad; atomic force microscopy; Diptera; pulvilli; secretion

1. INTRODUCTION

Numerous studies have been conducted to understand structure and function of the hairy attachment system of flies (Bauchhenss & Renner 1977; Bauchhenss 1979; Walker *et al.* 1985; Wigglesworth 1987; Beutel & Gorb 2001; Gorb 2001) and other animals that are able to walk on smooth vertical surfaces or ceilings. Up to now, the most precise adhesion measurements of the hairy attachment system have been performed for the gecko at the level of a bunch of terminal plates using a micro-electromechanical systems force sensor (Autumn *et al.* 2000). It has been shown previously that in the gecko system, Van der Waals interactions are responsible for strong attractive forces (Autumn *et al.* 2002). In insects, however, the basic physical forces contributing to overall adhesion may be completely different. Proposed hypotheses to explain the mechanism of insect attachment include a sticking fluid (Dewitz 1884), microsuckers (Simmermacher 1884) and electrostatic interaction (Gillett & Wigglesworth 1932). Experiments with beetles have strongly suggested that cohesive forces and molecular adhesion, mediated by pad secretion, may be involved in the mechanism of attachment (Stork 1983). When the hairy pads of the bug *Rhodnius prolixus* were treated with organic solvents, attachment was impaired (Edwards & Tarkanian 1970). In the aphid *Aphis fabae*, it was shown that, after walking on silica gel, the ability to attach to smooth surfaces was lost (Dixon *et al.* 1990). The final functional concept, however, for understanding the underlying physics of attachment in the hairy systems of insects is still missing.

The presence of fluids has been reported from hairy adhesive pads of reduviid bugs (Edwards & Tarkanian 1970), flies (Bauchhenss 1979; Walker *et al.* 1985) and coccinellid beetles (Ishii 1987). Thin-layer chromatography has shown that, in ladybird beetles (Coccinellidae), the chloroform-soluble part of the pad secretion consists mainly of hydrocarbons, fatty acids and alcohols (Ishii 1987). Gas chromatography has revealed that pad adhesive secretions consist of hydrocarbons and true waxes (Kosaki & Yamaoka 1996), corresponding well to the composition of the cuticle. Chemical extracts of tarsi of the beetle *Hemisphaerota cyanea* (Chrysomelidae, Cassidinae) or footprint material from glass surfaces to which the beetles had clung, yielded mixtures of saturated and unsaturated linear hydrocarbons of C_{20}–C_{28} chain length, with (*Z*)-9-pentacosene as the principal component. Recent data show that insect pad secretion is most probably an emulsion containing water-soluble and lipid-soluble fractions (Gorb 2001).

*Author and address for correspondence: Evolutionary Biomaterials Group, Max-Planck-Institute for Metals Research, Heisenbergstrasse 3, D-70569 Stuttgart, Germany (s.gorb@mf.mpg.de).

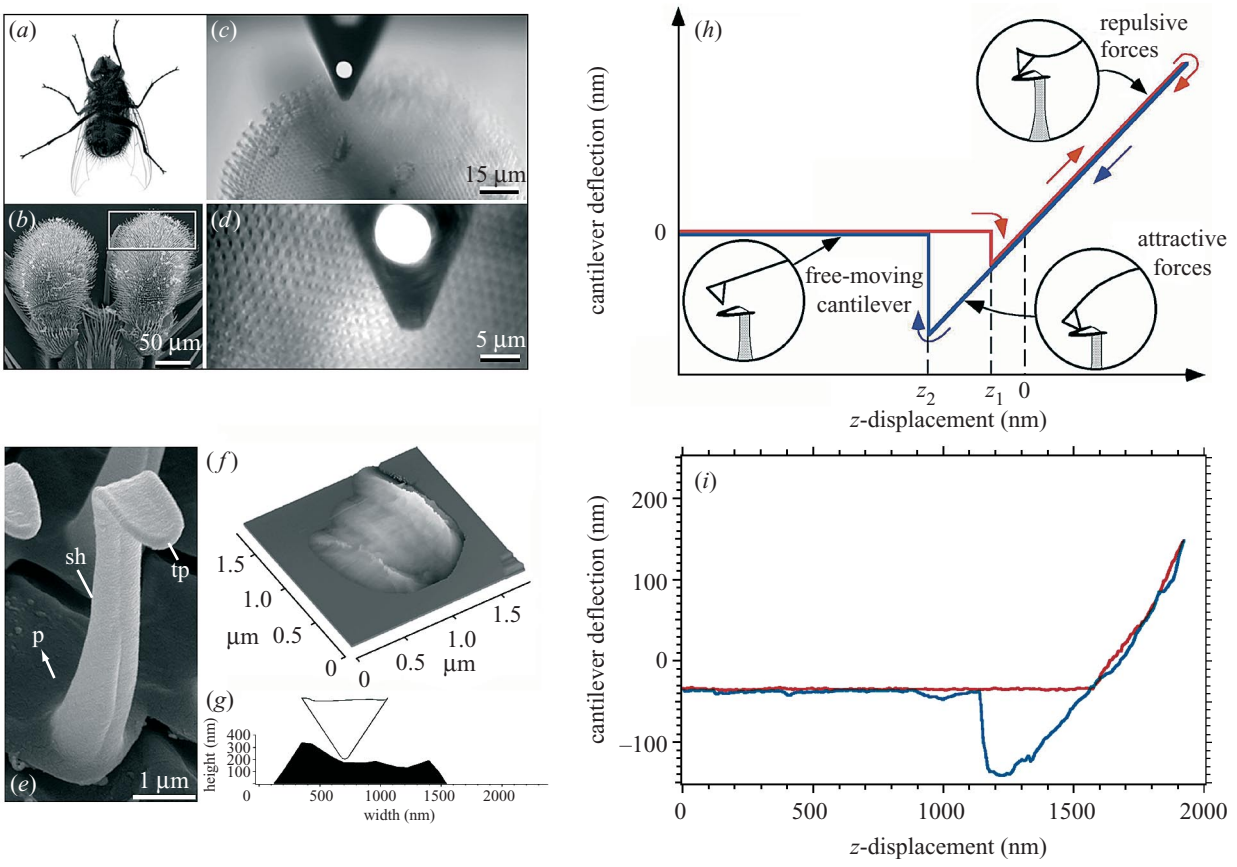

Figure 1. Force measurement performed on single terminal plates of the seta. (*a*) Fly *C. vicina* holding onto the ceiling (ventral aspect). (*b*) Fly attachment pads (pulvilli) covered with tenent setae (scanning electron micrograph, SEM). (*c*,*d*) Arrangement of triangular-shaped AFM cantilever with the reflected laser spot and pulvillus, as seen in the light microscope at different magnifications. (*e*) Single seta with the terminal plate at the apex (SEM). sh, setal shaft; p, proximal direction; tp, terminal plate. In the SEM, the border of the terminal plate appears to be higher compared with the centre of the plate. (*f*) AFM image recorded in the constant height-mode. The height profile reveals a higher position at the edge of the terminal plate. In this particular AFM-imaging mode, the feedback electronics were switched off. (*g*) Height profile of a terminal plate. To prevent imaging artefacts, as in the constant-height mode, a different AFM-imaging mode, reducing the lateral forces, was applied to the identical terminal plate: the force–volume imaging technique. This technique demonstrates that the border of the terminal plate is higher compared with the centre. For comparison, an AFM tip with a radius of 40 nm was inserted at the same scale. (*h*) Diagram of a force versus distance curve. Initially, the setal tip approaches the cantilever (left horizontal part of the curve). At sample position z_1, the cantilever jumps into contact with the setal plate surface, because of attractive forces. Approaching closer results in increasing repulsive forces, owing to the repulsion between the electrons of the interacting cantilever tip and seta atoms. At point 0, attractive and repulsive forces are balanced. After reaching the force set-point (right uppermost part of the curve), which is set by the experimenter, the setal plate is pulled back. At point z_2, where the maximum attractive force is measured, the AFM cantilever jumps from the contact. The force measured at point z_2 is the attractive force discussed in this paper. The difference between movement of the sample (z_2) and cantilever displacement (d(z_2)) at z_2 is referred to as the pull-off distance between tip and sample before the AFM tip jumps off. (*i*) A typical force versus distance curve measured on a single setal plate. The red line indicates the specimen approach; the blue line is the retraction process.

2. MATERIAL AND METHODS

(a) *Model of investigation*

Male and female imagines of *Calliphora vicina* Robineau-Desvoidy (Diptera, Brachycera) were taken from laboratory colonies at the MPI of Biological Cybernetics, Tübingen, and at the University of Würzburg (Germany). This species is a model for the study of hairy attachment pads and has been used in studies on pad ultrastructure and in the measurements of attachment forces.

(b) *Scanning electron microscopy*

The terminal tarsomere, together with the pulvilli, were fixed in 2.5% glutaraldehyde in phosphate-buffered saline (PBS; pH 7.3) and postfixed in osmium tetroxide. The preparations were then washed in PBS, dehydrated, transferred to absolute ethanol, and critical-point dried. After coating with gold–palladium (8 nm), the sections were viewed in a Hitachi S-800 scanning electron microscope at 20 kV.

(c) *Atomic force microscopy*

To investigate local attractive forces of single setae, a custom-made atomic force microscopy (AFM), equipped with a liquid chamber, was used (Langer *et al.* 1997, 2000). This instrument combines an AFM with an upright infrared differential interference contrast (DIC) video microscope (Axioskop FS; Zeiss, Germany) which allows proper positioning of the AFM tip and attachment pads (Langer *et al.* 2000) (figure 1*c*,*d*). The interaction between the AFM sensor and individual setal plates was detected by the so-called 'optical lever method' (Meyer & Amer 1988; Alexander *et al.* 1989). V-shaped Si3N4-microlevers, with pyramid-shaped tips, were used as AFM probes. The tips had a

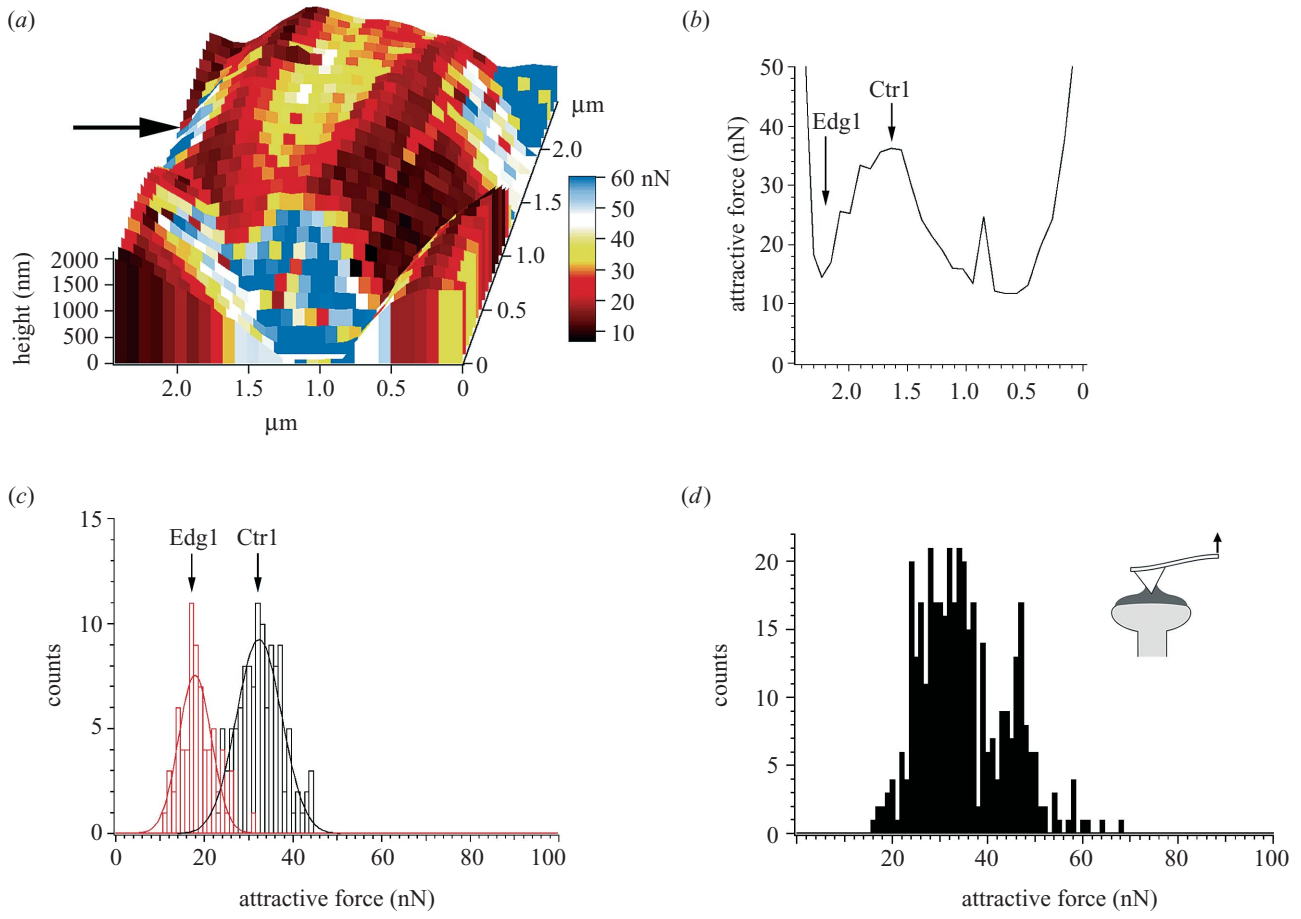

Figure 2. Local distribution of attractive forces on a single setal plate. (*a*) A three-dimensional attractive force image of a single terminal plate, measured in air. The colour encodes the local attractive force, whereas the height of the three-dimensional AFM image corresponds to surface topography. (*b*) Attractive force profile recorded on the top of the identical setal plate shown in (*b*). The arrows highlight the attractive forces measured at the edge (Edg1) and in the centre (Ctr1) of the setal plate. The attractive force is low at the edge (14.5 nN), and high in the centre (36.5 nN). (*c*) Histograms of the attractive forces of the identical terminal plate shown in (*a*). Edg1 highlights the forces measured at the border; Ctr1 shows the attractive forces measured in the centre of the terminal plate. Mean attractive force in the centre is significantly higher (33.0 ± 5.0 nN) than the attractive force at the edge (19.0 ± 4.0 nN). (*d*) Pooled attractive forces measured in the centres of five terminal plates; the median attractive force is 33.0 nN.

typical curvature radius of *ca.* 40 nm, and the cantilevers used had a typical spring constant of 0.5 N m^{-1} (Park Scientific Instruments, USA). Force constants of the AFM cantilevers were determined by the method of Cleveland *et al.* (1993). The measured force constants varied from 8.5×10^{-3} to 1.2×10^{-2} N m^{-1}. The approach of the AFM tip to individual hairs was controlled through the light microscope. For the local investigation of attractive forces, a piezoelectric tube scanner moved the AFM tip horizontally from point to point. At each point, the scanner stopped while the specimen was moved up and down at a frequency of 4 Hz and an amplitude of *ca.* 2 μm_{pp} (figure 1*e*,*f*). Terminal plates were studied at a resolution of 30 × 30 force versus distance curves (900 single tests). Measured attractive forces are presented as adhesion maps of the plate (figure 2*b*,*d*).

3. RESULTS

The attachment organs (pulvilli) of the fly are covered with setae (figure 1*a–d*), which consist of a shaft and terminal plate (figure 1*e*). In the fly *Calliphora vicina*, the terminal plate is oriented to the distal direction, and is responsible for contact with the substrate surface (Gorb 1998). The surface of this plate is slightly concave with a rounded, well-expressed edge (figure 1*f*,*g*).

Until now, it has been difficult, if not impossible, to record the adhesive forces on single setae of insect pads, because the area of interaction between the terminal plates and the substrate surface varied between the different measurements. Moreover, it was impossible to measure adhesive forces at a nanoNewton (nN) level and to allocate the measured force to a certain topographical point on the seta. Thus, it is not yet clear how the structure of single attachment setae and the corresponding interactive force mediate the attachment capability of the living animal.

AFM has opened the possibility of imaging surface structures with nanometric resolution and probing, very locally, the force interactions between a sharp tip and the submicroscopic area of a single terminal plate under various environmental conditions. In an initial experiment, the surface topography of individual attachment pads was investigated using AFM, by scanning the AFM tip at a constant height across the sample. The resulting image (figure 1*f*) revealed a heterogeneous surface morphology, with the border *ca.* 60 nm higher than the centre. Using this scanning mode, lateral forces could lead to an undesirable lateral displacement of the setal shaft. To prevent this artefact, a second AFM technique—the so-called 'force

versus distance measurement'—was used to image the surface topography of single attachment pads. This measurement allows local investigation of specimen topography, and the study of almost any type of force (either electrostatic or chemical) between the tip and terminal plate, with a high degree of accuracy. The surface is studied point-by-point rather than being scanned continuously line-by-line. Such an array of measurements provides information about the local attractive forces and/or surface topography. An entire measurement contains an array of force curves over the entire sample area and is generated by ramping the *z*-piezo as the tip scans across the area. Each force curve is measured at a unique *x*–*y* position in the area, and force curves from an array of *x*–*y* points are combined into a three-dimensional array of force data. The cantilever deflection is recorded with an accuracy of 1 nm, as a terminal plate approaches the AFM tip. The resulting force curve is plotted as a function of distance between the fixed end of the AFM cantilever and the specimen (figure 1*h*,*i*). For each recorded force curve, the maximum repulsive force (positive maximum in figure 1*h*), acting between tip and attachment pad, is kept constant at a given set-point using feedback-electronics. For each force curve, the position of the *z*-piezo, where the same repulsive force is reached, is plotted versus the corresponding *x*–*y* position on the terminal plate (figure 1*g*). Before the AFM tip moves to the next spot on the attachment pad, the sample is retracted, thus, preventing lateral forces. Using this technique, we were able to image the topography of a single attachment pad. As an example, a height profile is shown in figure 1*g*, where each point was measured at the same loading force of 0.8 nN. The border of 60–150 nm high around the terminal plate is clearly demonstrated by this method, supporting the result shown in figure 1*f*.

A second series of experiments examined the local adhesion on single attachment pads under ambient conditions (temperature: 295 K, humidity: 55%). Specimens were investigated within 20 min after preparation. Vertical movement of the *z*-piezo ranged from 0 to 2140 nm. Because the surfaces of the terminal plates studied are not homogeneous (figure 1*f*,*g*), it is of significant interest to collect an array of force curves, and look for local differences in adhesion. In addition to purely topographical information (figure 1*g*), the 'force versus distance measurement' provides information about local attractive forces acting between the AFM tip and the attachment pad. Attractive forces are measured while retracting the AFM tip from the terminal plate surface. The point of maximum attractive force is reached, when the stress, induced by the AFM cantilever, exceeds the attractive force. This situation corresponds to the point z_2 in figure 1*h*. These forces are plotted versus the corresponding *x*-*y* position on the terminal plate (figure 2*a*,*b*). Taking advantage of the simultaneous measurement of attractive forces and surface topography, figure 2*a* combines the height of the attachment pad, which is displayed as a three-dimensional surface plot, with the local attractive forces, presented on the surface plot as colour-coded pixels. Both the attractive force map in figure 2*a*, and the force profile in figure 2*b*, confirm higher local adhesion in the centre of the attachment pad (labelled Ctr1) and lower adhesion at the border (labelled Edg1). Attractive forces, measured on the edge and in the centre of the attachment pad, are displayed in figure 2*a*, and plotted as histograms in figure 2*c*. Only those data points, where the AFM tip itself, rather than the lateral surface of the pyramidal AFM tip, contact the terminal plate, were taken into account. The higher forces, between scan ranges 2.4–2.0 and 0.4–0.0 μm (figure 2*b*), were due to a higher contact area between the AFM tip and the plate. These forces were not used for data analysis. Although the edge reveals a significantly smaller median attractive force of 19.0 nN, the centre shows a median force of 33.0 nN ($T = 2652$, $p < 0.001$, Mann–Whitney rank sum test). A median attractive force of 33.0 nN was measured in the centre of five individual terminal elements from five different flies, investigated within 20 min after preparation.

In summary, the topography of the attachment pad is heterogeneous with the border being 60–150 nm higher than the centre. The attractive forces in the centre (median force = 33.0 nN) are *ca*. 1.7 times higher than the attractive forces measured at the border. We still do not know, however, the mechanism of measured adhesion. This issue will be addressed in the following experiments.

In the gecko, it has been shown that an individual seta operates by Van der Waals forces (Autumn *et al.* 2002); in insects, pad fluid is involved in adhesion (Bauchhenss 1979; Walker *et al.* 1985). The effect of the pad fluid on adhesion was tested by comparing the attractive force, on a clean glass cover-slip (temperature: 295 K, relative humidity: 55%), with the attractive force on an identical glass cover-slip covered with footprints of pad secretion from the fly *C. vicina*. Force versus distance measurements were performed testing the adhesion on the supporting glass cover-slip and single drops of pad fluid. Within 20 min after preparation, high attractive forces (35.0 ± 3 nN) were measured on the drop of pad fluid, and low forces (11.5 ± 2.0 nN) on the glass cover-slip (figure 3*a*,*d*). Adhesion measurements were repeated several times on the same area of the glass cover-slip. Even after 5 min, the attractive forces on the pad fluid dropped from 35.0 nN (figure 3*d*) to 23.5 nN (figure 3*e*); after an additional 5 min they had decreased to 18.0 nN (figure 3*f*). This decrease in attractive force, measured on a single drop of pad fluid, correlates very well over time with a decrease in drop size (see figure 3*a*–*c*). This is probably a result of evaporation reducing the size of the secretion drops over time. As the secretion drops get smaller, the effective contact area between the AFM tip and pad fluid decreases, resulting in lower attractive forces.

How do these attractive forces, measured on footprints, correlate with attractive forces measured on single terminal plates of the fly? For comparison, attractive forces from three terminal plates were pooled and displayed in a histogram (figure 3*h*). For analysis, only those measurements were used where the drop diameter was in the range of 1 μm, corresponding to a single droplet from a single attachment pad. All drops showing a larger diameter in the AFM image are probably the result of the fusion of many droplets formed during the attachment process. The median attractive force on single drops of pad secretion was 38.5 nN (figure 3*h*), corresponding very well to the attractive forces detected in the centre of the plates (figure 2*d*). Measurements on footprints attached to a glass cover-slip showed that the forces are acting over a long distance—from 48 to 212 nm (figure 3*i*). The median distance

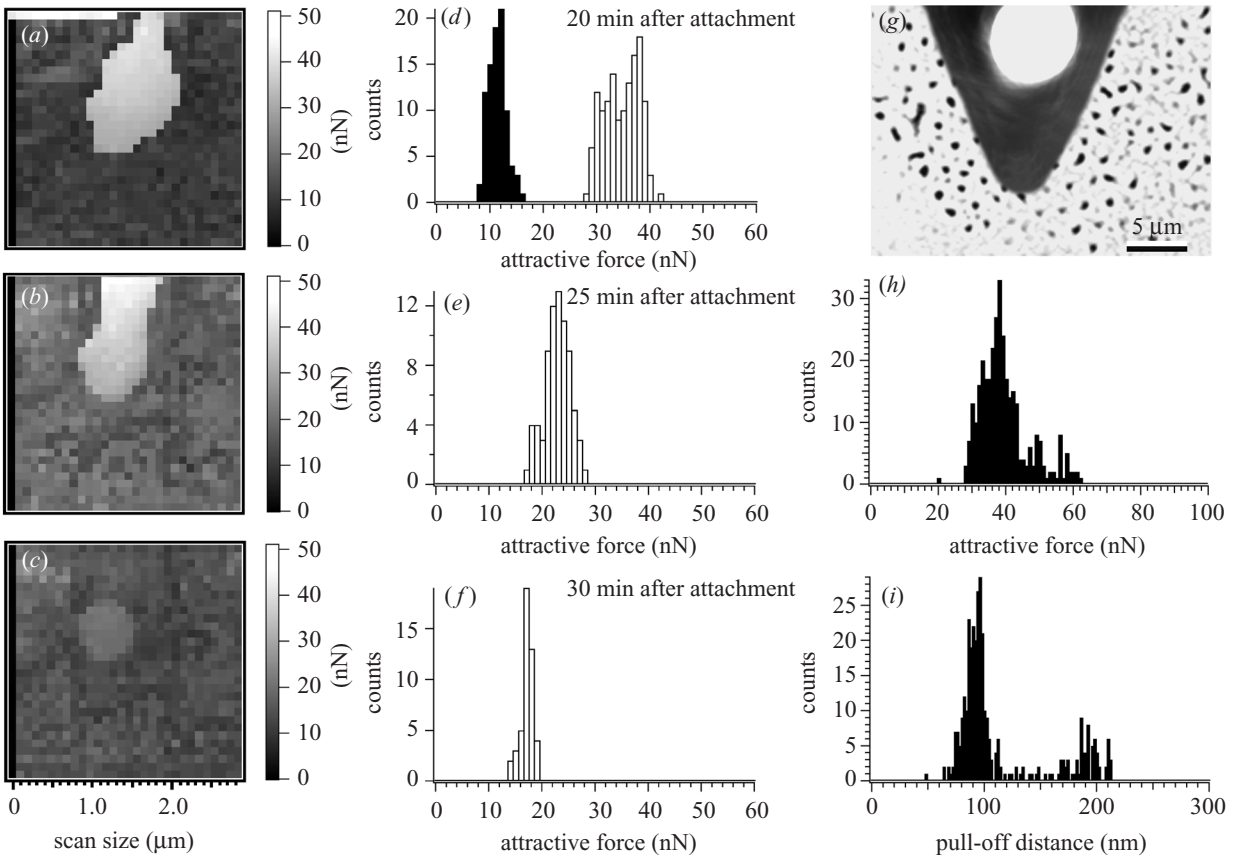

Figure 3. Force–volume imaging on single secreted droplets over a period of 30 min. (*a–c*) Adhesion maps recorded on a single drop 20, 25, and 30 min after attachment of the fly seta on a clean glass cover-slip. The bright areas correspond to high adhesion, measured on a single secretory drop. The drop size clearly decreases with increasing time. (*d–f*) Frequency histograms of the attractive forces on the clean glass surface (solid bars in (*d*)), on the droplet after 20 min (clear bars in (*d*)), on the same droplet after 25 min (*e*), and after 30 min (*f*). The highest attractive force is on the top of the droplet, and the lowest on the clean glass surface. (*g*) Image of the experimental situation, as seen under the light microscope. (*h,i*) Pooled attractive forces (*h*), and pull-off distances (*i*) from three droplets investigated within 20 min after attachment. The median attractive force (38.5 nN) corresponds well with the high attractive forces measured in the centre of attachment pads. The median pull-off distance (96.0 nm), measured on the identical droplets, is well beyond the short-range Van der Waals forces.

between the sample and tip, where the cantilever broke the contact, was 96.0 nm. Such high pull-off distances were observed only when the cantilever was in contact with the pad secretion; the median pull-off distance on the supporting glass cover-slip was much smaller (25 nm).

The importance of secretory fluid for adhesion in flies is demonstrated by the consistent results in the attractive forces measured in the centre of the plates and on single drops, the decrease in attractive force with decreasing drop size, and long pull-off distances, detectable only on single secretion drops.

The effect of buffer solution on adhesion is also of interest. In an initial experiment, drops of footprints attached to a glass surface were observed in air using a phase-contrast light microscope (figure 4*a*). Treatment of the identical preparation with buffer solution, containing 1.3 mM $CaCl_2$, 5.8 mM KCl, 144 mM NaCl, 0.9 mM $MgCl_2$, 0.7 mM NaH_2Po_4 5.6 mM D-glucose and 10 mM HEPES (figure 4*b*), removed the footprints. The use of this preparation was repeated for setae of flies. After filling the specimen chamber with the buffer solution, an AFM tip was manoeuvred towards a single terminal plate, controlled through the light microscope. Terminal plates were investigated in the same way, as shown in figure 1*h*. Detected attractive forces were pooled and plotted in a histogram (red histogram in figure 4*c*). A comparison with the attractive forces obtained on the seta under ambient conditions (black bars) shows that treatment with buffer solution dramatically reduces the median attractive force by a factor of *ca.* 9—from 33.0 to 3.5 nN.

4. DISCUSSION

A change in the environment from air to a buffer solution may have different contributing effects to the overall attractive force measured on a single attachment pad. As shown by Xu *et al.* (1997), the force interaction between a silicon nitride tip (as used in our experiments) and a silicon nitride sample depends on the liquid environment. Replacement of pure water by a 0.5 mM KCl electrolyte solution resulted in long-range repulsive forces that were not detected in pure water. Long-range repulsion is generally attributed to charges that reside on the surfaces. The origin of these charges can be either the dissociation of surface molecule groups or the adsorption of ions to the surface. This long-range repulsive force may be one explanation for the reduction in attractive forces observed in our measurements on attachment pads in buffer solution. The removal of capillary force is another possible

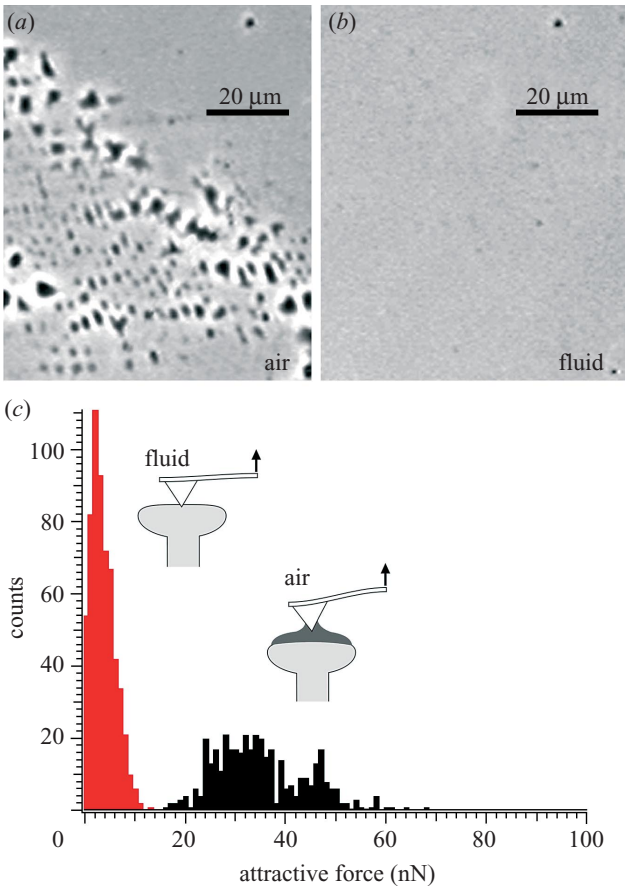

Figure 4. (*a*) Phase-contrast light microscopy was used to control the effect of buffer solution on the drops of secretion covering the setal plates. Pad prints were attached to a glass surface and imaged in air. (*b*) The same preparation, imaged in air, after treatment with buffer solution. The droplets disappeared. (*c*) Attractive forces measured on terminal plates before and after treatment with buffer solution. Adhesion is highly dependent on the presence of pad secretion. The red histogram displays pooled attractive forces on different plates in an aqueous environment. The black histogram displays the attractive forces on terminal plates in air before treatment. Treatment with buffer solution reduced the median attractive force from 33.0 to 3.5 nN.

explanation of low attraction in an electrolyte. Although contributing significantly to the overall attractive force under ambient conditions (Schenk *et al.* 1998), capillary forces are reduced in a liquid environment. Moreover, we have shown that secretion fluid is dissolved in buffer solution (figure 4*b*), indicating that the low attractive forces shown in figure 4*c* are due to the interaction of the AFM tip with the solid material of the plate rather than with the secretory fluid.

5. CONCLUSION

There is strong evidence, from all AFM results, that pad secretion, which contributes mainly to the adhesion of fly setae, is located at the centre of the attachment pad. Time after seta preparation is critical for proper adhesion measurement, because evaporation of the pad secretion fluid results in smaller attractive forces (figure 3*a–c*). The absence of pad secretion in buffer indicates that, at least one component of secretion is water-soluble, emphasizing the importance of environmental conditions in understanding the mechanism of fly adhesion. Although Van der Waals interaction cannot be completely excluded from the fly adhesion process, secretion-mediated capillary forces seem to play a major role in the generation of strong adhesion between the single terminal plate and the substrate.

M. Heusel (MPI of Biological Cybernetics, Tübingen, Germany) and K. Scheller (University of Würzburg, Germany) kindly supplied *Calliphora vicina*. V. Kastner made linguistic corrections, which improved an earlier draft of the manuscript. This research was supported by the Federal Ministry of Science of Germany (BMBF) grant BioFuture 0311851 to S. G., the Deutsche Forschungs Gemeinschaft (DFG) grant LA 1227/1-3, and by the Federal Ministry of Science Germany (BMBF) grant Nanobiotechnology 0312017A to M.L.

REFERENCES

Alexander, S., Hellemans, L., Marti, O., Schneir, J., Ellings, V., Hansma, P. K., Longmire, M. & Gurley, J. 1989 An atomic-resolution atomic force microscope implemented using an optical lever. *J. Appl. Phys.* **65**, 164–167.

Autumn, K., Liang, Y. A., Hsieh, S. T., Zesch, W., Chan, W. P., Kenny, T. W., Fearing, R. & Full, R. J. 2000 Adhesive force of a single gecko foot hair. *Nature* **405**, 681–685.

Autumn, K., Sitti, M., Liang, Y. A., Peattie, A. M., Hansen, W. R., Sponberg, S., Kenny, T. W., Fearing, R., Israelachvili, J. N. & Full, R. J. 2002 Evidence for van der Waals adhesion in gecko setae. *Proc. Natl Acad. Sci. USA* **99**, 12 252–12 256.

Bauchhenss, E. 1979 Die Pulvillen von *Calliphora erythrocephala* Meig. (Diptera, Brachycera) als Adhäsionsorgane. *Zoomorphologie* **93**, 99–123.

Bauchhenss, E. & Renner, M. 1977 Pulvillus of *Calliphora erythrocephala* Meig. (Diptera; Calliphoridae). *Int. J. Insect Morphol. Embryol.* **6**, 225–227.

Beutel, R. & Gorb, S. N. 2001 Ultrastructure of attachment specializations of hexapods (Arthropoda): evolutionary patterns inferred from a revised ordinal phylogeny. *J. Zool. Syst. Evol. Res.* **39**, 177–207.

Cleveland, J. P., Manne, S., Bocek, D. & Hansma, P. K. 1993 A nondestructive method for determining the spring constant of cantilevers for scanning force microscopy. *Rev. Sci. Instrum.* **64**, 403–405.

Dewitz, H. 1884 Über die Fortbewegung der Tiere an senkrechten glatten Flächen vermittels eines Sekretes. *Arch. Ges. Physiol.* **33**, 440–481.

Dixon, A. F. G., Croghan, P. C. & Gowing, R. P. 1990 The mechanism by which aphids adhere to smooth surfaces. *J. Exp. Biol.* **152**, 243–253.

Edwards, J. S. & Tarkanian, M. 1970 The adhesive pads of Heteroptera: a re-examination. *Proc. R. Entomol. Soc. Lond.* A **45**, 1–5.

Gillett, J. D. & Wigglesworth, V. B. 1932 The climbing organ of an insect, *Rhodnius prolixus* (Hemiptera, Reduviidae). *Proc. R. Soc. Lond.* B **111**, 364–376.

Gorb, S. N. 1998 The design of the fly adhesive pad: distal tenent setae are adapted to the delivery of an adhesive secretion. *Proc. R. Soc. Lond.* B **265**, 747–752. (doi:10.1098/ rspb.1998.0356)

Gorb, S. N. 2001 *Attachment devices of insect cuticle*. Dordrecht, The Netherlands: Kluwer Academic.

Ishii, S. 1987 Adhesion of a leaf feeding ladybird *Epilachna vigintioctomaculata* (Coleoptera: Coccinellidae) on a vertically smooth surface. *Appl. Entomol. Zool.* **22**, 222–228.

Kosaki, A. & Yamaoka, R. 1996 Chemical composition of footprints and cuticula lipids of three species of lady beetles. *Jpn. J. Appl. Entomol. Zool.* **40**, 47–53.

Langer, M. G., Öffner, W., Wittmann, H., Flösser, H., Schaar, H., Häberle, W., Pralle, A., Ruppersberg, J. P. & Hörber, J. K. H. 1997 A scanning force microscope for simultaneous force and patch-clamp measurements on living cell tissues. *Rev. Sci. Instrum.* **68**, 2583–2590.

Langer, M. G., Koitschev, A., Haase, H., Rexhausen, U., Hörber, J. K. H. & Ruppersberg, J. P. 2000 Mechanical stimulation of individual stereocilia of living cochlear hair cells by atomic force microscopy. *Ultramicroscopy* **82**, 269–278.

Meyer, G. & Amer, N. 1988 Novel optical approach to atomic force microscopy. *Appl. Phys. Lett.* **53**, 1045–1047.

Schenk, M., Füting, M. & Reichelt, R. 1998 Direct visualization of the dynamic behavior of a water meniscus by scanning electron microscopy. *J. Appl. Phys.* **84**, 4880–4884.

Simmermacher, G. 1884 Untersuchungen über Haftapparate an Tarsalgliedern von Insekten. *Z. Wiss. Zool.* **40**, 481–556.

Stork, N. E. 1983 A comparison of the adhesive setae on the feet of lizards and arthropods. *J. Nat. Hist.* **17**, 583–597.

Walker, G., Yule, A. B. & Ratcliffe, J. 1985 The adhesive organ of the blowfly, *Calliphora vomitoria*: a functional approach (Diptera: Calliphoridae). *J. Zool. Lond.* **205**, 297–307.

Wigglesworth, V. B. 1987 How does a fly cling to the under surface of a glass sheet? *J. Exp. Biol.* **129**, 363–367.

Xu, W., Blackford, B. L., Cordes, J. G., Jericho, M. H., Pink, D. A., Levadny, V. G. & Beveridge, T. 1997 Atomic force microscope measurements of long-range forces near lipid-coated surfaces in electrolytes. *Biophys. J.* **72**, 1404–1413.

As this paper exceeds the maximum length normally permitted, the authors have agreed to contribute to production costs.